

Cite this: *Energy Environ. Sci.*,
2023, 16, 2338

Lab free protein-based moisture electric generators with a high electric output†

Renbo Zhu,^a Yanzhe Zhu,^a Long Hu,^{*a} Peiyuan Guan,^{id a} Dawei Su,^{id b}
Shuo Zhang,^a Chao Liu,^a Ziheng Feng,^a Guangyu Hu,^a Fandi Chen,^a Tao Wan,^{id *a}
Xinwei Guan,^a Tom Wu,^{id a} Rakesh Joshi,^{id a} Mengyao Li,^{id a}
Claudio Cazorla,^{id *c} Yuerui Lu,^{id d} Zhaojun Han,^{*e} Haolan Xu^{id f} and
Dewei Chu^{id a}

Moisture–electric generators (MEGs), harvesting ubiquitous moisture from the environment for electricity generation, have attracted great interest as power supply devices. However, there are great challenges associated with material availability, fabrication accessibility and operation environment, which are key factors to achieve high output with low cost for practical applications, and a deeper understanding of the underlying mechanism of interactions between MEGs and water is urgently required. Here, a whey protein available in supermarkets is used to fabricate low-cost MEGs with controllable performance through tuning surface charges and hydrophilicity, which provides new insights into the electricity generation mechanism and large-scale application. The MEGs exhibit the highest voltage output of 1.45 V at a room humidity level of 40% relative humidity. The whey protein films possess the merits of low cost (70 times cheaper than commonly used polymers), being flexible and semi-transparent, and having self-healing ability, presenting excellent comprehensive device performance. Besides, MEGs can operate well at extreme temperatures (–20 °C or 50 °C) and power a location tracker in a desert with 26% relative humidity. The modified functional layers with selective ion absorption and controllable outputs provided a deeper understanding of electricity generation in MEGs and demonstrated great potential in powering a wide range of electronic devices in various dynamic environments with high sustainability and reliability.

Received 10th March 2023,
Accepted 28th March 2023

DOI: 10.1039/d3ee00770g

rsc.li/ees

Broader context

The increasing demand of green and sustainable energy booms the development of electricity generation with energy sources available in the environment. The operation environment (e.g., sunlight and mechanical motion) of photovoltaics and piezoelectric or triboelectric nanogenerators impedes the practical application of traditional nanogenerators. Moisture–electric generators (MEGs) are promising candidates for the wide application of energy harvesting as moisture is an abundant energy source in the environment. However, the reported MEGs still show insufficient electric outputs at room humidity as well as being high cost for device fabrication. In this regard, we fabricated a protein-based MEG from cheap ordinary materials used in daily life. The protein-based MEG delivers the highest continuous voltage output at room humidity (1.45 V at 45% relative humidity) with the lowest cost (17.61 AUD m^{–2}). Besides, the high electric output makes MEGs capable of powering a wide range of practical devices under extreme conditions (–20 °C to 50 °C and < 40% relative humidity). Moreover, protein-based MEGs achieve selective ion absorption and controllable outputs by modification of surface charges. Their hydrophilicity is also explored with surface plasma treatment for achieving enhanced hydrophilicity and higher outputs. This work paves the way for practical applications of MEGs and a deeper understanding of electricity generation in MEGs.

Introduction

The development of new energy conversion technologies such as photovoltaics¹ and piezoelectric² or triboelectric³ nanogenerators

is sought-after to satisfy the enormous demand for electric power including applications of electrocatalysis and electronics. Since moisture is ubiquitous in the natural environment and a paramount medium for energy transfer in the Earth's climate, it can

^a School of Materials Science and Engineering, University of New South Wales, Sydney, NSW 2052, Australia. E-mail: long.hu@unsw.edu.au, tao.wan@unsw.edu.au^b School of Mathematical and Physical Sciences, University of Technology Sydney, Sydney, NSW 2007, Australia^c Departament de Física, Universitat Politècnica de Catalunya, Campus Nord B4-B5, E-08034 Barcelona, Spain. E-mail: claudio.cazorla@upc.edu^d College of Engineering and Computer Science, Australian National University, Canberra, ACT 2601, Australia^e School of Chemical Engineering, University of New South Wales, Sydney, NSW 2052, Australia. E-mail: zhaojun.han@unsw.edu.au^f Future Industries Institute, University of South Australia, Adelaide, SA 5095, Australia† Electronic supplementary information (ESI) available. See DOI: <https://doi.org/10.1039/d3ee00770g>

be a tremendous energy source and produce around 60×10^{15} W per year, which is several orders of magnitude larger than the average electricity consumption by human activities. Recently, moisture electric generators (MEGs) that can directly convert chemical potential energy from moisture into electricity have been identified as a promising technology for implementation in self-powered devices.⁴⁻⁶

The unique advantages of MEGs include the great availability of moisture, zero by-product, and no need for temperature variation and mechanical movement.⁷⁻¹⁰ In the past few years, remarkable progress in polymer-based MEGs has been made through employing various strategies such as designing bilayer structure,⁶ utilizing synergistic effect¹¹ and introducing high-valent charge carrier.¹² However, the high costs of materials and facilities involved in MEG fabrication further limit the large-scale production of MEGs for isolated off-grid applications including self-sustained systems and mobile electronics, making MEGs infeasible for applications in our daily life.^{4,5,13-16} Additionally, most

reported MEGs as power supply devices exhibit excessively sensitive humidity dependence and low and transient power output. The unsatisfactory voltage output (<1 V) and undesirable transient (several seconds) current output at low relative humidity (RH) limit their practical application.¹⁷ Therefore, it is essential to develop large-scale practical applications of MEGs with balanced merits of being cost-effective with easy accessibility and all-region applicable with a high electric output under extreme environmental conditions.

In this work, we fabricated functional layers in MEGs from whey protein as whey protein is a highly available source in nature with extremely low cost and contains abundant hydrophilic functional groups that are beneficial for moisture absorption.^{18,19} Whey protein costs 0.08 AUD g^{-1} , which is 70 times lower than the commonly used polymers (*e.g.*, poly(4-styrenesulfonic acid) and poly dimethyl diallyl ammonium chloride). Besides, surface charges and hydrophilicity of whey protein were modified on a large-scale by engineering its pH

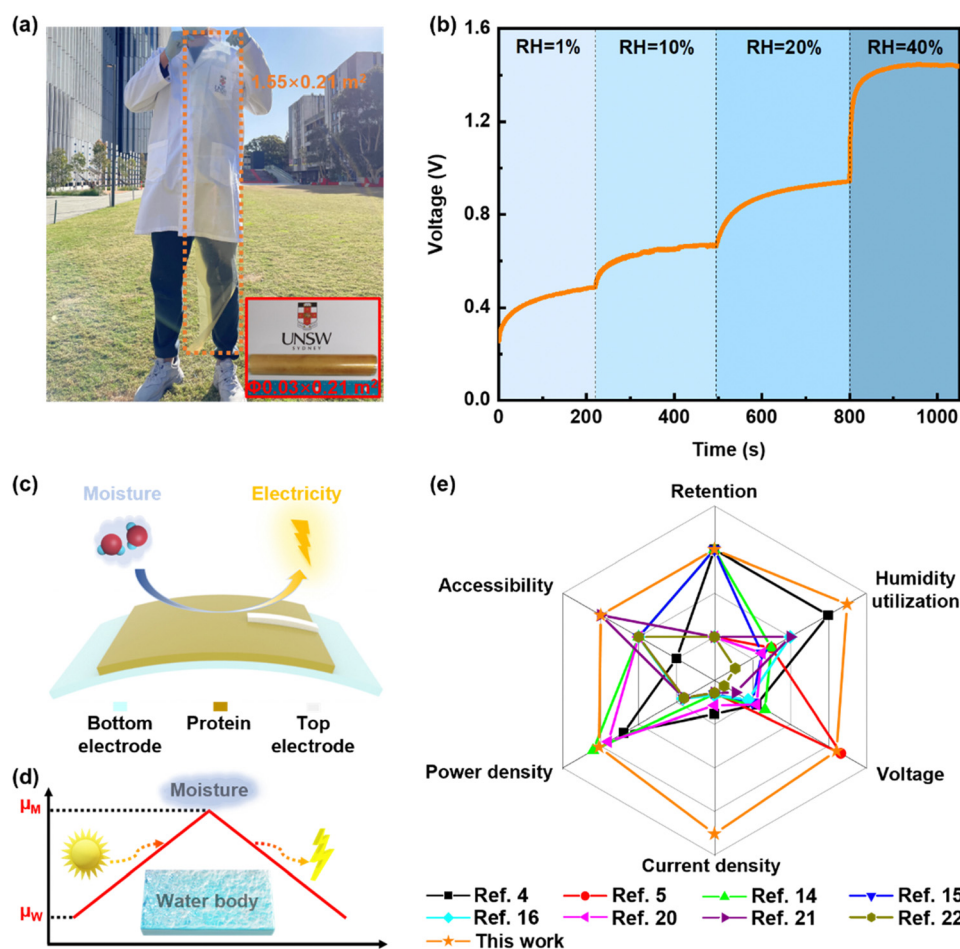


Fig. 1 Illustration of whey protein film for MEGs. (a) Photograph of a large size free-standing protein film with a full size of $1.55 \times 0.21 \text{ m}^2$ and a folded size of $\Phi 0.03 \times 0.21 \text{ m}^2$. (b) Voltage output of MEGs at different RH levels with CNTs and FTO glasses as top and bottom electrodes, respectively. (c) Schematic illustration of the absorbing moisture for electricity generation by MEGs. (d) Illustration of energy conversion between the water body and moisture for electricity generation. The difference in chemical potential between water (μ_W) and moisture (μ_M) drives electricity generation. (e) Comparison of comprehensive performance based on recently reported MEGs. The MEGs with a transient output show shorter retention than MEGs with a continuous output. The power density is calculated with voltage and current density. The humidity utilization (100%-RH) is calculated from RH that generates the highest voltage output.

value and surface post-treatment, respectively. The MEGs fabricated from whey protein deliver an ultra-high voltage of 1.45 V (highest value at room humidity) and a current density of $113 \mu\text{A cm}^{-2}$ (100 times higher than that of the previously reported protein-based MEG⁴) at RH = 40%. Moreover, we first designed a lab-free high-performance MEG working under extreme conditions such as in deserts with an extremely low humidity (1.05 V at 26% RH), which successfully powered a wireless location tracker in a desert. This work solves a series of current challenges of MEGs, which advances MEGs into a new stage for large-scale practical applications.

Results and discussion

The obtained free-standing protein film with a size of $1.55 \times 0.21 \text{ m}^2$ ($\Phi 0.03 \times 0.21 \text{ m}^2$ for the folded film) is the largest protein film for MEGs (Fig. 1a), and is semi-transparent and can be easily tailored and assembled for large-scale and low-cost applications.

Protein-based MEGs with fluorine-doped tin oxide (FTO) glasses, protein films, and carbon nanotubes (CNTs) as bottom electrodes, functional layers, and top electrodes, respectively, exhibit voltages of 1.45 V, 0.95 V, 0.67 V, and 0.49 V at RHs of 40%, 20%, 10%, and 1%, respectively (Fig. 1b and Fig. S3, ESI[†]). Among the RH levels, 10% is comparable to a desert environment. The voltage output reaches 1.45 V with a current output of $113 \mu\text{A cm}^{-2}$ at RH = 40% (Fig. S3, ESI[†]), which are the highest electric outputs^{4,5,14–16,20–22} ever reported for MEGs operating at room humidity level (Table S1, ESI[†]). The voltage output monotonously increases with the RH, which is also confirmed in the measurements with dry N_2 (Fig. S4, ESI[†]). The MEGs can absorb more water at higher RH levels, which harvests more chemical potential energy from the moisture and leads to higher electric outputs.^{20,23} The scanning electron microscopy (SEM) image shows that the protein film exhibits a porous structure with a thickness of $\sim 292 \mu\text{m}$ (Fig. S5, ESI[†]), thus facilitating water absorption for electricity generation (Fig. 1c). About 50% of absorbed solar energy on earth drives water body into moisture²⁴ and leads to

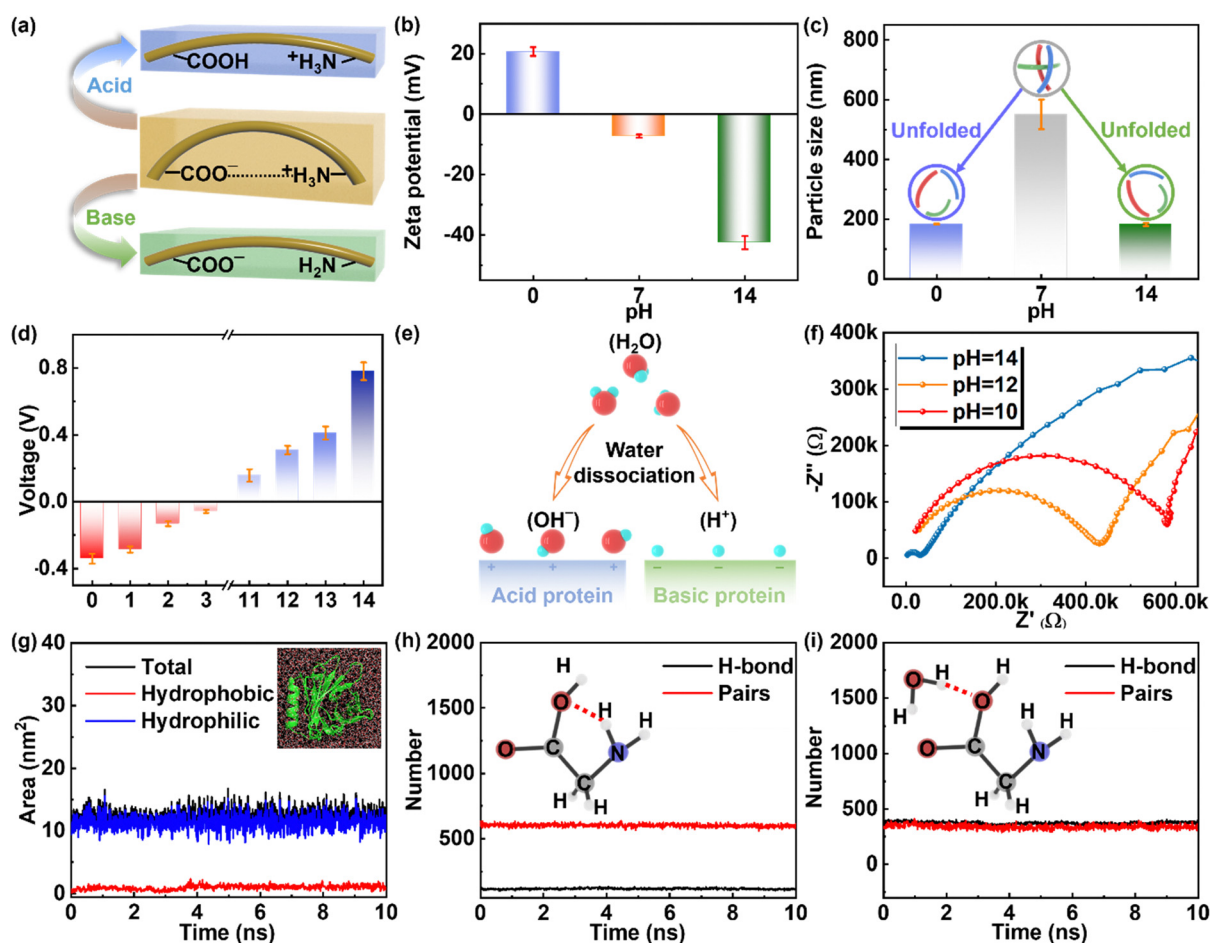


Fig. 2 Surface charge modification of the whey protein films. (a) The illustration of the modified surface functional groups with either acid or basic solution. (b) Zeta charge potential of the 1 wt% whey protein dispersion with different pH values. (c) Particle sizes of 1 wt% whey protein in water solvent with different pH levels. (d) Voltage output of protein films fabricated by protein dispersions with different pH values. (e) Schematic illustration of electricity generation of acid and basic protein films exposed to moisture. (f) EIS of protein films fabricated with different pH levels. (g) Solvent accessible surface area over time extracted from the molecular dynamics simulation. (h) Number of intra protein hydrogen bonds over time. (i) Number of hydrogen bonds between the protein and solvent over time.

the increased chemical potential of water (μ_W and μ_M for water body and moisture, respectively, in Fig. 1d). MEGs absorb water from moisture by a hydrophilic functional layer and generates electricity by the chemical potential gradient between μ_W and μ_M . In this work, a protein-based MEG shows excellent comprehensive performance in retention (continuous voltage), humidity utilization, voltage, current density, power density and material accessibility (Fig. 1e and Table S1, ESI[†]), which was enabled using the multiple strategies as elucidated later.

The pH environment is known to significantly modify the surface charges of protein or deconstruct protein structures,^{25–28} and thus tuning the pH values represents an effective approach towards electricity generation as surface charges of protein are capable of absorbing opposite ions for charge separation. As shown in Fig. 2a, the surface charges of protein are presumably negative under basic conditions since the added OH^- would react with the $-\text{COOH}$ of the whey protein, thus leading to the formation of negative charges ($-\text{COO}^-$) on protein surfaces due to H^+ removal. On the other hand, the surface potential is positive under acid conditions since the added H^+ would react with $-\text{NH}_2$ to form $-\text{NH}_3^+$ groups, thus resulting in positive surface charges. As confirmed by zeta potential results, the basic and acid proteins achieve negatively (-42.6 mV) and positively (20.7 mV) charged surfaces (Fig. 2b), respectively, which also indicated the exposed $-\text{COO}^-$ in the basic protein and $-\text{NH}_3^+$ in the acid protein, respectively. Besides, the decreased particle size of whey protein in acid or basic solution (Fig. 2c) also indicates that hydrogen bonds break to deconstruct large protein clusters and unfold protein molecules, and more functional groups are exposed to achieve water absorption and charge separation, which are beneficial for electricity generation. Additionally, a small amount of poly(ethylene glycol) (PEG) was added as a plasticizer²⁹ to improve the strength and uniformity of protein films for a continuous voltage output (0.78 V for 28 h in Fig. S6, ESI[†]).

To investigate the effect of pH values of protein solution on MEG device performance, we fabricated MEGs with a structure of FTO/protein/CNTs based on the protein films with controlled addition of potassium hydroxide (KOH) or hydrochloric acid (HCl). As shown in Fig. 2d, the voltage output of MEGs is negative for acid protein films and positive for the basic protein films (CNT is the negative and positive electrode, respectively). Notably, the basic protein achieves a much higher absolute voltage than that of the acid protein (0.78 V and -0.34 V for protein with pH = 14 and 0, respectively without plasma treatment), which is attributed to the higher zeta potential of basic protein with greater charge separation and electricity generation. Besides, the voltage and zeta potential (Fig. S7, ESI[†]) of protein mixed with sodium hydroxide (NaOH) or potassium chloride (KCl) also indicate that the surface potential adjusted by pH, instead of the addition of various ions, leads to a high voltage output. Different types of widely used whey protein are also investigated, and Fig. S8 (ESI[†]) shows a similar voltage output and zeta potential, which underscores the universality of whey protein as the functional layer for electricity generation. The contact potential difference

(CPD) of the protein surface also indicates that basic protein films exhibit more positive surface charges (Fig. S9, ESI[†]).

The charged protein surface absorbs ions with opposite charges from water dissociation ($\text{H}_2\text{O} \leftrightarrow \text{OH}^- + \text{H}^+$),³⁰ and leads to a vertical ion gradient and voltage output for charge separation and electricity generation (Fig. 2e and Fig. S10, ESI[†]). The increased concentration of OH^- from water dissociation absorbed on the acid protein surface with a lower pH value leads to the formation of enhanced negative electric potential because of more positive surface charges introduced by HCl modification. Similarly, the increased concentration of H^+ absorbed on the basic protein surface leads to the formation of a positive electric potential because of more exposed $-\text{COO}^-$ groups in the basic protein with a higher pH. Therefore, the absolute maximum voltage (V_{max}) of basic and the acid protein film increases with the addition of KOH and HCl, which originates from the more surface charges of basic protein films with high pH and acid protein films with low pH, respectively. To further confirm this, the electrochemical impedance spectroscopy (EIS) of the basic protein was collected. The results imply that the conductivity of basic protein film increases with the pH of protein dispersion (Fig. 2f), suggesting that the protein dispersion solution with higher pH values leads to the accumulation of protein surface charges. MEGs show a high vertical voltage output with no obvious horizontal voltage output (Fig. S11, ESI[†]), which also demonstrates that the vertical water gradient and ion gradient contribute to electricity generation. The water gradient is attributed to the MEG heterostructure with the top side exposed to the moisture and the bottom side isolated from the moisture, respectively. With distilled water dropped on the protein surface, the MEGs exhibit a lower voltage output and a higher current output (0.25 V and 1.86 mA cm^{-2} in Fig. S12, ESI[†]), which result from the lower vertical water gradient and film resistance, respectively, as a greater amount of water permeates into the bottom side of the protein film with a lower water gradient by water drops. However, more water absorption from water drops contributes to the better conductivity of the protein film, which generates a higher current output. The electricity generation by water gradient is also verified by the higher voltage output of MEGs with a thicker protein film (Fig. S13, ESI[†]) as the water gradient increased with the film thickness.⁷ The MEGs with different electrode materials show a similar voltage output in the ambient environment without the involvement of a chemical reaction (Fig. S14, ESI[†]), which excludes the role of the electrochemical reaction and relative electrode positions for electricity generation.

Molecular modelling was also investigated to illustrate the interaction of whey protein and water molecules. The β -lactoglobulin protein, the main component of whey protein, is stable in the water solvent as calculated by the molecular dynamics simulation (Fig. 2g). The root-mean-square deviations (RMSDs) of atomic positions relative to the crystal structure and equilibrated system are shown in Fig. S15a (ESI[†]). Both time series show that the RMSD levels off to ~ 0.08 nm, indicating that the structure is stable. Although the value for the radius of gyration R_G is fluctuating

between 1.17 and 1.25 and RG_y is fluctuating between 1.20 and 1.28 after 8 ns, the reasonably invariant RG values (around 1.5 nm) indicate that the β -lactoglobulin proteins in the water solution remain stable, retaining its compact (folded) form over a duration of 10 ns at 300 K (Fig. S15b, ESI[†]).

The solvent accessible surface area (SASA) of β -lactoglobulin over time is shown in Fig. 2g. The fluctuation of the hydrophobic areas is around 1 nm², while that of the hydrophilic areas is much larger at around 12 nm². The hydrophobic and hydrophilic SASA values over time remain very constant. This suggests the superior proton conductivity *via* the hydrophilic residues, and meanwhile the small hydrophobic residues maintain the existence of the moisture gradient, benefiting the long duration of the continuous electric power in the ambient environment. This conclusion is further confirmed by the data of SASA per residue (Fig. S15c, ESI[†]). In Fig. 2h, the intra-hydrogen bond number fluctuates around 110 over time, which remains quite stable. However, the number of pairs within 0.35 nm is significantly larger (~ 600), suggesting more possibility of forming a water chain around intra- β -lactoglobulin protein and transporting the protons. The number of bonds connecting protein to solvent hydrogen is around 370 with a fluctuation of 20 to 40 over time (Fig. 2i), which indicates a stability level similar to the intra-hydrogen bonds. The number of hydrogen bonds within 0.35 nm is closer to the overall hydrogen bond count (~ 330). The less hydrogen bonds between intra protein and solvent further confirm that the β -lactoglobulin protein structure promotes the formation of the moisture gradient and the generation of the electric potential.

Since the basic protein films achieved much higher voltages than the acidic ones, we used the basic protein films for MEG

applications in the following. Plasma treatment, as an effective post-treatment tool to modify surface hydrophilicity, has been extensively employed in previous works of surface treatment.^{31–33} To make the protein films more hydrophilic, plasma treatment was applied to basic protein films after drying the protein film on the substrate. As shown in Fig. 3a, V_{\max} values of MEGs are 0.78 V, 1.15 V, and 1.45 V after plasma treatment with durations of 0 h, 2 h, and 4 h, respectively. Clearly, plasma treatment significantly improves the voltage output of MEGs, which is also demonstrated in devices made from whey proteins of other brands (Fig. S16, ESI[†]). Although the plasma treatment required a vacuum, the control experiment indicates that vacuum drying applied on protein films makes no contribution to the increased voltage in the MEGs (Fig. S17, ESI[†]).

To investigate the origins of improved voltage output, X-ray photoelectron spectroscopy (XPS) measurements were conducted to analyze surface chemical states. According to XPS data, the O/C ratio increases from 1.07 to 1.68 after 4 h of plasma treatment (Fig. 3b and Fig. S18, ESI[†]), suggesting that oxidation of protein molecules occurred during plasma treatment. The high energy plasma and the remaining oxygen can effectively break C–C bonds and contribute to the surface oxidation of protein films.³³ Moreover, sodium dodecyl sulfate-polyacrylamide gel electrophoresis (SDS-PAGE) patterns are widely used to separate proteins with different molecular masses.^{34,35} The SDS-PAGE patterns of whey protein with and without reduction (break disulfide bonds to better separate protein molecules) also indicate that oxidation of the protein occurred in the plasma treatment as the weight of protein molecules increases after plasma treatment (Fig. 3c), which contributes to the increased oxygen-based groups and greater

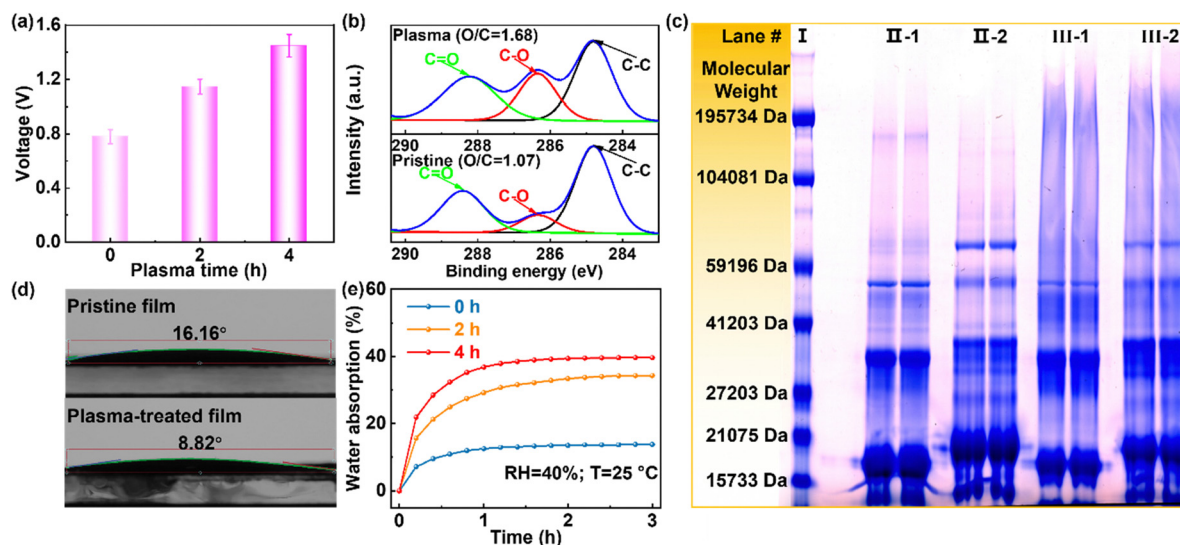


Fig. 3 Hydrophilicity modification of the whey protein films by plasma treatment. (a) The voltage output of the protein films at RH = 40%. The protein surface is treated by plasma with different durations. (b) XPS spectra of the film surfaces with and without plasma treatment for 4 h. (c) SDS-PAGE patterns of the whey protein with and without plasma treatment for 4 h. The patterns I, II-1, II-2, III-1, and III-2 are prestained markers, non-reducing pristine protein, reducing pristine protein, non-reducing plasma-treated protein, and reducing plasma-treated protein, respectively. (d) The water contact angles of the protein films with and without plasma treatment for 4 h. (e) The water absorption of plasma-treated protein films at RH = 40% and $T = 25$ °C.

hydrophilicity on the protein surfaces. Additionally, almost identical Fourier-transform infrared (FTIR) spectra of the protein films with and without plasma treatment were observed (Fig. S19, ESI[†]), which further validated that the surface functional groups (*e.g.*, amide and amid) were not noticeably altered. As with the beneficial effect of plasma treatment, the improved O/C ratio is expected to make the protein surface more hydrophilic, which was verified by the water contact angle measurements, *i.e.*, the contact angle decreased from 16.16° to 8.82° after the plasma treatment (Fig. 3d). The water absorption of protein films with a plasma treatment of 0 h, 2 h and 4 h is 13.75 wt%, 34.26 wt% and 39.60 wt%, respectively (Fig. 3e), which also indicates that the plasma treatment remarkably enhanced the ability of water absorption in the protein films to absorb more water from the environment for electricity generation, thus making the strategy applicable under low relative humidity conditions such as in deserts.

Protein-based MEGs can be easily assembled into integrated devices to widen their practical applications. The arrays were fabricated with CNTs as bottom electrodes, basic protein films as functional layers, and Ag paste as top electrodes. The flexible MEG arrays could be easily attached to fabrics or hands and no deterioration of performance was observed after 1000 bending tests (Fig. S20, ESI[†]), which indicates great potential in wearable applications. A commercial calculator was successfully powered at room humidity by a MEG array of 3 units in series (Fig. S21, ESI[†]). When the load resistance increases, the voltage output of the external load increases, while the current output decreases, which leads to the highest power of 1.16 μW (11.6 $\mu\text{W cm}^{-2}$) with a load resistance of 0.1 $\text{M}\Omega$ (Fig. S22, ESI[†]). Besides, the MEGs were charged at a room humidity of 40% and then discharged with a current of 10 μA as an operation cycle, and exhibit good stability in the repeated operation (Fig. S23, ESI[†]). The electric output of MEGs can be

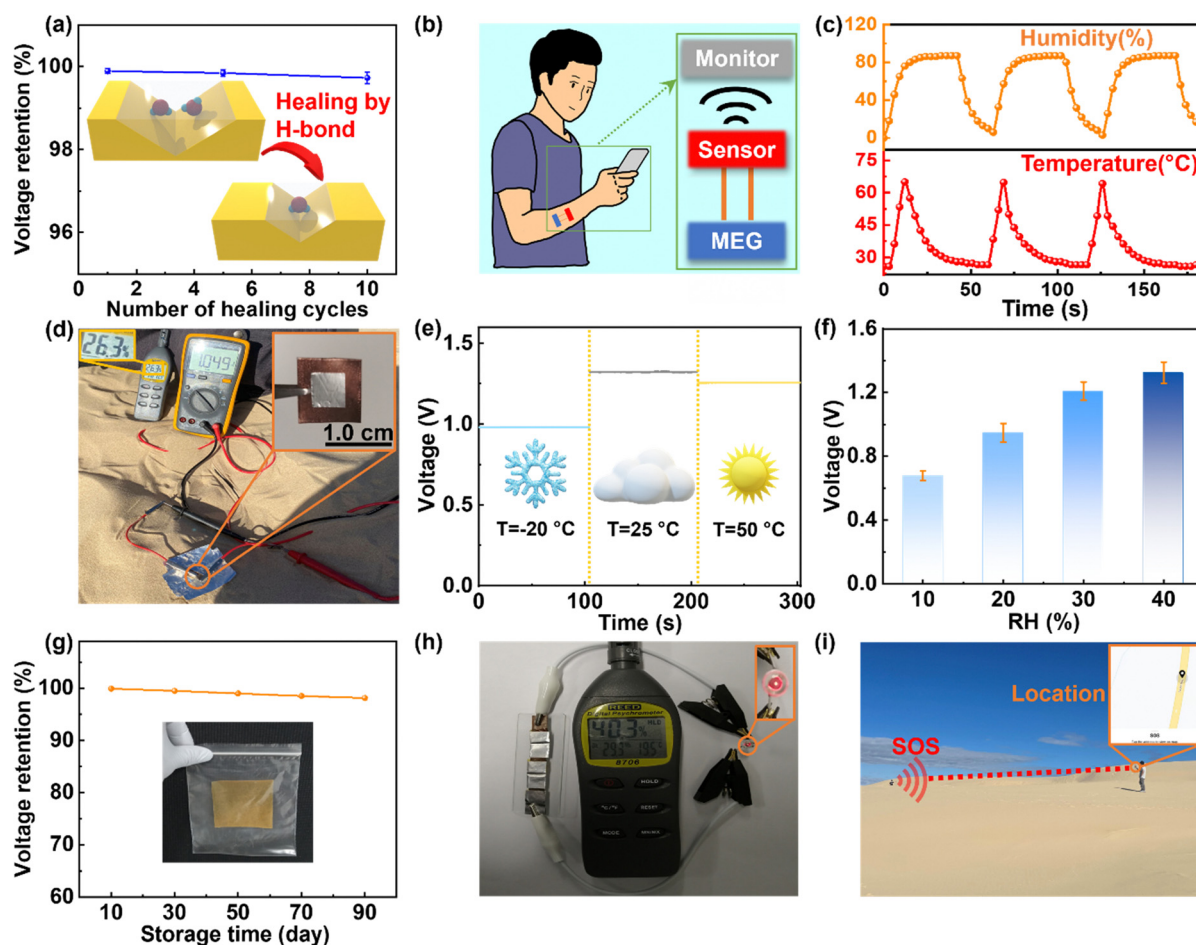


Fig. 4 Application demonstration of protein-based MEGs as power supply devices. (a) V_{max} of protein films with different healing cycles. (b) Illustration of device integration for wearable and wireless sensor applications. (c) Output of wireless humidity and temperature sensors powered by a 0.01 F capacitor with 3.5 V, charged by 16 MEG units at room humidity. The humidity and temperature around sensors are controlled with different values to imitate different environments. (d) Photograph of a lab-free MEG with a voltage output of 1.05 V in a desert with RH = 26%. The Cu/protein/Al MEGs are fabricated with $0.8 \times 0.8 \text{ cm}^2$ Cu/protein and $0.5 \times 0.5 \text{ cm}^2$ Al. (e) Voltage output of lab-free MEGs at different humidity levels at 25 °C. (f) The voltage output of the lab-free MEGs at different humidity levels at 25 °C. (g) Voltage of the protein film without plasma treatment after different durations of storage. (h) Red light-emitting diode light powered directly by 3 units in series with RH = 40%. (i) Operation photograph of a wireless location tracker with a mobile phone and 0.01 F capacitor. The tracker is powered by the charged capacitor and transmits immediate location information to the mobile phone.

scaled up by connecting multiple MEG units in series or parallel, as shown in Fig. S24 (ESI†). The voltage and current output increase linearly with the numbers of MEG units connected in series and parallel, respectively, which indicates great potential in powering practical electronic devices that require high electric power.

Moreover, the protein films exhibit self-healing ability to sustain a high electric output. The protein films were scratched with a knife and then distilled water was added dropwise on the scratches. After drying the scratched film at 50 °C for 6 h, the electric output of the protein film (Fig. 4a) almost recovered (99.6% of the initial V_{\max} after 10 healing cycles). The damaged structure of the protein film is almost fully recovered, as shown in the optical images (Fig. S25a, ESI†). The absorbed water bridged the edges of scratched protein *via* hydrogen bonds between the functional groups of protein and absorbed water (Fig. S25b, ESI†). The protein films were healed after adjacent functional groups were connected directly by hydrogen bonds,^{36,37} thus showing no obvious V_{\max} decline. Besides, the protein-based MEGs in this work could also generate electricity to charge commercial capacitors (Fig. S26, ESI†) and power wireless electronic devices, such as wireless sensors (Fig. 4b and Fig. S27, ESI†). Wireless humidity/temperature sensors reliably operated and transmitted humidity and temperature signals to the monitor (Fig. 4c). The integrated system paves the way for self-powered data monitoring with remote wireless communications.

Since the pre-prepared protein films achieved superior performance with a low RH *via* extremely simple fabrication processes, this technology would make MEGs accessible to civilians living in a wide range of conditions, particularly in extreme regions such as off-grid desert areas. We chose a desert located in the New South Wales state in Australia and brought a plastic bag containing pre-prepared protein films and daily-life materials such as Cu and Al foil for the field fabrication of MEGs (Fig. 4d and Movie S1, ESI†). The MEGs were easily available (lab-free MEGs) and generated a high voltage output (1.05 V) in an extremely dry environment (RH = 26.3% in the tested desert). Moreover, the MEG delivered an open-circuit voltage of 1.32 V (31.56 V g^{-1}) and $56.53 \text{ } \mu\text{A}$ (1.35 mA g^{-1}) at room humidity (40% RH), as shown in Fig. S28 and S29 (ESI†). The MEG with protein, Cu and Al as a functional layer, bottom electrode, and top electrode costs 17.61 AUD m^{-2} , which is cheap and accessible for civilian application. Besides, lab-free MEGs are demonstrated to work under extreme outdoor conditions with a dynamic variation of temperatures (Fig. 4e) and exhibit voltages of 0.98 V ($T = -20 \text{ } ^\circ\text{C}$), 1.32 V ($T = 25 \text{ } ^\circ\text{C}$) and 1.25 V ($T = 50 \text{ } ^\circ\text{C}$), respectively. The water content is greater at higher temperatures, which contributes to an increased voltage output from $-20 \text{ } ^\circ\text{C}$ to $25 \text{ } ^\circ\text{C}$. However, the protein film exhibits lower water absorption at higher temperatures, which leads to a decreased voltage output from $25 \text{ } ^\circ\text{C}$ to $50 \text{ } ^\circ\text{C}$. As shown in Fig. 4f, our devices achieved voltages of 1.32 V, 1.21 V, 0.95 V, and 0.68 V at RH levels of 40%, 30%, 20%, and 10%, respectively. As shown in Fig. S30 (ESI†), the area with a RH higher than 80% only covers 10% of the Australian land, suggesting

that most currently reported MEGs are not applicable to achieving high performance. Fortunately, our MEGs can work well at a RH lower than 40%, which significantly enhances the feasibility of the technology. Since Australia is one of the driest lands in the world, the MEGs reported in this work should operate well in most areas around the world.

Additionally, to verify the stability of the protein films, the same batch of basic protein films was stored in a sealed plastic bag (25 °C and 40% RH) and then their MEG performance was tested after different durations of storage. As shown in Fig. 4g, the MEG devices without plasma treatment achieved stable performance over a long storage time (97.8% V_{\max} remained after 3 months of storage). Through simply assembling units in series, lab-free MEGs could also charge commercial capacitors and power practical electronic devices. The red light-emitting diode (LED) was powered directly at room humidity by 3 MEG units connected in series (Fig. 4h and Movie S2, ESI†), which illustrates great potential as a direct power source in ambient environment. Besides, a capacitor of 0.01 F with 3.5 V charged by 4 units at 26% RH in the desert (RH = 26%) could power an electronic location tracker. Fig. 4i shows that the wireless tracker (Movie S3, ESI†) could send immediate location information to a monitor, even in the dry desert, which provides a facile approach for location tracking in urgent situations.

Conclusions

In summary, we have developed protein-based, low-cost ($\sim 8.81 \text{ AUD m}^{-2}$) MEGs from protein sources commonly accessible in daily life. The semi-transparent protein-based MEGs achieved outputs of 1.45 V and $113 \text{ } \mu\text{A cm}^{-2}$ at room humidity (40% RH), which is the highest voltage so far for MEGs operating at room humidity. This outstanding performance can be attributed to the modifications of surface charges and hydrophilicity achieved in this work. It is demonstrated that the voltage output of protein-based MEGs can be tuned from -0.34 V to 0.78 V by adjusting the pH values of the protein dispersion. Plasma treatment was also proved to be an effective approach to increase the electric output (0.78 V to 1.45 V after 4 h plasma treatment) by surface oxidation and hydrophilicity modification of the protein films. The protein-based MEGs exhibited excellent self-healing ability and great flexibility. Moreover, the free-standing protein film was integrated with ordinary materials (Cu/protein/Al) for lab-free MEGs and could be stored for over three months without obvious output decline, which powered an LED light and wireless location tracker successfully. Thus, the protein-based MEGs presented in this work exhibit excellent comprehensive performance, which makes them accessible to civilians for practical applications.

Author contributions

R. Z., S. Z., C. L., Z. F., and G. H performed device fabrication. Y. Z., M. L., Tao W., and X. W. carried out characterization.

D. S. and C. C. performed molecular dynamics simulation. L. H., Tom W., R. J., Y. L., Z. H., H. X., and D. C. supervised the project. P. G. and F. C. helped with graph modification. R. Z. and D. S. wrote the paper. All authors reviewed and approved the final manuscript.

Conflicts of interest

There are no conflicts to declare.

Acknowledgements

The authors acknowledge the financial support from the Australian Research Council Projects LP210200495, LP190100829, and DP210100879.

Notes and references

- L. Hu, Q. Zhao, S. Huang, J. Zheng, X. Guan, R. Patterson, J. Kim, L. Shi, C. H. Lin, Q. Lei, D. Chu, W. Tao, S. Cheong, R. D. Tilley, A. W. Y. Ho-Baillie, J. M. Luther, J. Yuan and T. Wu, *Nat. Commun.*, 2021, **12**, 1–9.
- M. M. Yang, Z. D. Luo, Z. Mi, J. Zhao, S. P. E and M. Alexe, *Nature*, 2020, **584**, 377–381.
- Z. L. Wang, *Adv. Energy Mater.*, 2020, **10**, 1–6.
- X. Liu, H. Gao, J. E. Ward, X. Liu, B. Yin, T. Fu, J. Chen, D. R. Lovley and J. Yao, *Nature*, 2020, **578**, 550–554.
- Y. Huang, H. Cheng, C. Yang, P. Zhang, Q. Liao, H. Yao, G. Shi and L. Qu, *Nat. Commun.*, 2018, **9**, 4166.
- H. Wang, Y. Sun, T. He, Y. Huang, H. Cheng, C. Li, D. Xie, P. Yang, Y. Zhang and L. Qu, *Nat. Nanotechnol.*, 2021, **16**, 811–819.
- J. Tan, S. Fang, Z. Zhang, J. Yin, L. Li, X. Wang and W. Guo, *Nat. Commun.*, 2022, **13**, 1–8.
- H. Wang, T. He, X. Hao, Y. Huang, H. Yao, F. Liu, H. Cheng and L. Qu, *Nat. Commun.*, 2022, **13**, 1–11.
- H. Zhu, J. Mao, Y. Li, J. Sun, Y. Wang, Q. Zhu, G. Li, Q. Song, J. Zhou, Y. Fu, R. He, T. Tong, Z. Liu, W. Ren, L. You, Z. Wang, J. Luo, A. Sotnikov, J. Bao, K. Nielsch, G. Chen, D. J. Singh and Z. Ren, *Nat. Commun.*, 2019, **10**, 1–8.
- M. Han, H. Wang, Y. Yang, C. Liang, W. Bai, Z. Yan, H. Li, Y. Xue, X. Wang, B. Akar, H. Zhao, H. Luan, J. Lim, I. Kandela, G. A. Ameer, Y. Zhang, Y. Huang and J. A. Rogers, *Nat. Electron.*, 2019, **2**, 26–35.
- J. Bai, Y. Huang, H. Wang, T. Guang, Q. Liao, H. Cheng, S. Deng, Q. Li, Z. Shuai and L. Qu, *Adv. Mater.*, 2021, 2103897.
- Z. Sun, L. Feng, X. Wen, L. Wang, X. Qin and J. Yu, *Mater. Horiz.*, 2021, **8**, 2303–2309.
- F. Zhao, H. Cheng, Z. Zhang, L. Jiang and L. Qu, *Adv. Mater.*, 2015, **27**, 4351–4357.
- Y. Huang, H. Cheng, C. Yang, H. Yao, C. Li and L. Qu, *Energy Environ. Sci.*, 2019, **12**, 1848–1856.
- H. Cheng, Y. Huang, F. Zhao, C. Yang, P. Zhang, L. Jiang, G. Shi and L. Qu, *Energy Environ. Sci.*, 2018, **11**, 2839–2845.
- T. Xu, X. Ding, C. Shao, L. Song, T. Lin, X. Gao, J. Xue, Z. Zhang and L. Qu, *Small*, 2018, **14**, 1–7.
- D. Shen, W. W. Duley, P. Peng, M. Xiao, J. Feng, L. Liu, G. Zou and Y. N. Zhou, *Adv. Mater.*, 2020, **2003722**, 1–31.
- M. Peydayesh and R. Mezzenga, *Nat. Commun.*, 2021, **12**, 1–17.
- T. Ben-Arye, Y. Shandalov, S. Ben-Shaul, S. Landau, Y. Zagury, I. Ianovici, N. Lavon and S. Levenberg, *Nat. Food*, 2020, **1**, 210–220.
- D. Shen, M. Xiao, G. Zou, L. Liu, W. W. Duley and Y. N. Zhou, *Adv. Mater.*, 2018, **30**, 1–8.
- X. Gao, T. Xu, C. Shao, Y. Han, B. Lu, Z. Zhang and L. Qu, *J. Mater. Chem. A*, 2019, **7**, 20574–20578.
- W. Yang, X. Li, X. Han, W. Zhang, Z. Wang, X. Ma, M. Li and C. Li, *Nano Energy*, 2020, **71**, 104610.
- F. Zhao, Y. Liang, H. Cheng, L. Jiang and L. Qu, *Energy Environ. Sci.*, 2016, **9**, 912–916.
- A. H. Cavusoglu, X. Chen, P. Gentine and O. Sahin, *Nat. Commun.*, 2017, **8**, 617.
- W. Ma, A. Saccardo, D. Roccatano, D. Aboagye-Mensah, M. Alkaseem, M. Jewkes, F. Di Nezza, M. Baron, M. Soloviev and E. Ferrari, *Nat. Commun.*, 2018, **9**, 1–9.
- H. S. Chung, S. Piana-Agostinetti, D. E. Shaw and W. A. Eaton, *Science*, 2015, **349**, 1504–1510.
- G. Yildiz, J. Andrade, N. E. Engeseth and H. Feng, *J. Colloid Interface Sci.*, 2017, **505**, 836–846.
- E. V. Shtykova, L. A. Dadinova, N. V. Fedorova, A. E. Golanikov, E. N. Bogacheva, A. L. Ksenofontov, L. A. Baratova, L. A. Shilova, V. Y. Tashkin, T. R. Galimzyanov, C. M. Jeffries, D. I. Svergun and O. V. Batishchev, *Sci. Rep.*, 2017, **7**, 1–16.
- L. Bekale, D. Agudelo and H. A. Tajmir-Riahi, *Colloids Surf., B*, 2015, **130**, 141–148.
- M. Li, L. Zong, W. Yang, X. Li, J. You, X. Wu, Z. Li and C. Li, *Adv. Funct. Mater.*, 2019, **29**, 1–8.
- G. Xue, Y. Xu, T. Ding, J. Li, J. Yin, W. Fei, Y. Cao, J. Yu, L. Yuan, L. Gong, J. Chen, S. Deng, J. Zhou and W. Guo, *Nat. Nanotechnol.*, 2017, **12**, 317–321.
- Y. Tao, Z. Wang, H. Xu, W. Ding, X. Zhao, Y. Lin and Y. Liu, *Nano Energy*, 2020, **71**, 104628.
- X. Liu, Y. Cheng, C. Liu, T. Zhang, N. Zhang, S. Zhang, J. Chen, Q. Xu, J. Ouyang and H. Gong, *Energy Environ. Sci.*, 2019, **12**, 1622–1633.
- E. M. Kofoed and R. E. Vance, *Nature*, 2011, **477**, 592–597.
- A. Sonn-Segev, K. Belacic, T. Bodrug, G. Young, R. T. VanderLinden, B. A. Schulman, J. Schimpf, T. Friedrich, P. V. Dip, T. U. Schwartz, B. Bauer, J. M. Peters, W. B. Struwe, J. L. P. Benesch, N. G. Brown, D. Haselbach and P. Kukura, *Nat. Commun.*, 2020, **11**, 1–10.
- T. Xu, X. Ding, Y. Huang, C. Shao, L. Song, X. Gao, Z. Zhang and L. Qu, *Energy Environ. Sci.*, 2019, **12**, 972–978.
- A. Pena-Francesch, H. Jung, M. C. Demirel and M. Sitti, *Nat. Mater.*, 2020, **19**, 1230–1235.